Science Advances

AAAS

advances.sciencemag.org/cgi/content/full/2/9/e1601017/DC1

Supplementary Materials for

Polymyxins and quinazolines are LSD1/KDM1A inhibitors with unusual structural features

Valentina Speranzini, Dante Rotili, Giuseppe Ciossani, Simona Pilotto, Biagina Marrocco, Mariantonietta Forgione, Alessia Lucidi, Federico Forneris, Parinaz Mehdipour, Sameer Velankar, Antonello Mai, Andrea Mattevi

Published 9 September 2016, *Sci. Adv.* **2**, e1601017 (2016)
DOI: 10.1126/sciadv.1601017

This PDF file includes:

Supplementary Materials and Methods

Cell viability. Cell viability assays were performed seeding MV4-11 in 96-well plate followed by treatment in triplicate with increasing concentrations of inhibitor compounds (range 15-100000 nM). Plates were then incubated at 37ºC with 5% CO_2 for 4 days. On day 4, Alamar Blue (Life Technologies) was added to the cells and, after 3 hours incubation, its fluorescence was detected using a TECAN Freedom Evo plate reader (540-570 nm excitation wavelength, 580-610 nm emission wavelength, Tecan Trading AG, Switzerland). Percentage of viability of treated cells relative to vehicle was calculated as following: % of cell viability = (average of the triplicates for each treated sample – average background signal) / (average of the triplicates of the vehicle control sample – average background signal).

Cell growth analysis. MV4-11 cells were grown in RPMI supplemented with 10% FBS serum, 2 mM L-glutamine and antibiotics, treated with the desired compounds, and counted after 24 hours, 3 days, and 5 days of treatment with trypan blue.

Transcriptional analysis: quantitative PCR. Total RNA was purified using RNeasy Mini Kit (Qiagen, Valencia, CA), quantified and reverse transcribed. 5-10 ng of cDNA were used to perform quantitative PCR (qPCR) using SYBR Green Reaction Mix (Perkin Elmer, Boston, MA). Gfi1-B mRNA level was normalized against rPPO mRNA.

Immunoblotting. MV4-11 cells were treated at different concentrations (200 nM and 1 μM) of **MC2694**, **E11**, **MC2580** and polymyxin E. Whole cell lysates were subjected to SDS-PAGE, and then

immunoblotted using antibodies against different histone modifications (H3K4me2, H3K9me2, and H3 – Abcam, Cambridge, UK).

PDB search of stacking ligands. The whole Protein Data Bank was searched to identify protein-ligand complexes with stacking assemblies similar to compounds **E11** and **MC3767**. Initial criteria were set as follows: 1) more than 3 copies of the same ligand had to be in the active site, 2) the ligand had to have more than 10 non-hydrogen atoms, 3) the ligands had to be within 4 Å from protein residues and 4) the ligand had not to be one of the most common cofactors, identified by none of the three letter codes 'HEM' (Fe-containing protoporphirin IX, heme), 'HEC' (heme C), 'BCL' (bacteriochlorophyll A) , 'FAD' (flavin-adenine dinucleotide), 'NAD' (nicotinamide-adenine dinucleotide), 'CLA' (chlorophyll A), 'NDP' (NADPH dihydro-nicotinamide-adenine dinucleotide phosphate). This search returned 599 hits, whose structures were examined individually, resulting in overall reduction to 13 by removal of: 1) non-drug candidates (lipids, detergents, vitamins, polymers, dyes, co-factors, sugars, buffer molecules, AMP, GMP, analogs and derivatives), 2) single-copy ligands found in multimeric biological assemblies, 3) ligands modeled in multiple conformations, and 4) crystallization artifacts (inferred both by PDB analysis and by original work comments).

G9a inhibition by MC2694. Inhibition of human G9a by **MC2694** was measured following the protocol described in **(*37*)**.

Chemistry of E11, MC2694, MC3767, MC4120, MC4121. Melting points were determined on a Stuart™ melting point apparatus SMP10. ^{1}H-NMR spectra were recorded at 400 MHz using a Bruker AC 400 spectrometer; chemical shifts are reported in δ (ppm) units relative to the internal reference tetramethylsilane (Me_4Si). Microwave-assisted reactions were performed with a Biotage Initiator™

(Uppsala, Sweden) high frequency microwave synthesizer working at 2.45 GHz, fitted with magnetic stirrer and sample processor; reaction vessels were Biotage microwave glass vials sealed with applicable cap; temperature was controlled through the internal IR sensor of the microwave apparatus. Mass spectra were recorded on an API-TOF Mariner by Perspective Biosystem (Stratford, Texas, USA), samples were injected by a Harvard pump using a flow rate of 5−10 μL/min, infused in the Electrospray system. All compounds were routinely checked by TLC and ^{1}H-NMR. TLC was performed on aluminum-backed silica gel plates (Merck DC, Alufolien Kieselgel 60 F_{254}) with spots visualized by UV light or using a $KMnO_4$ alkaline solution. All solvents were reagent grade and, when necessary, were purified and dried by standard methods. Concentration of solutions after reactions and extractions involved the use of a rotary evaporator operating at reduced pressure of ~ 20 Torr. Organic solutions were dried over anhydrous sodium sulfate. All chemicals were purchased from Sigma Aldrich s.r.l., Milan (Italy) or from TCI Europe N.V., Zwijndrecht (Belgium), and were of the highest purity. As a rule, samples prepared for physical and biological studies were dried in high vacuum over P_2O_5 for 20 hours at temperatures ranging from 25 to 40°C, depending on the sample melting point.

Compound **MC2694** was prepared as previously reported **(*37*)**. Compounds **E11** and **MC3767** were synthesized in two steps starting from the corresponding 2,4-dichloro-6,7-dimethoxyquinazoline **1**, which was prepared according to the procedure described in literature **(*38*).** Nucleophilic substitution using the proper commercial amine nucleophiles gave access to the 4-substituted 2-chloroquinazoline intermediates **MC4120** and **MC4121**, which were further heated with commercially available 3-(dimethylamino)propylamine under microwave irradiation to afford the target 2,4-diamino-quinazolines compounds **E11** and **MC3767**.

*Preparation of N4-(1-benzylpiperidin-4-yl)-N2-(3-(dimethylamino)propyl)-6,7-dimethoxyquinazoline-2,4-diamine (**E11**).* 4-Amino-1-benzylpiperidine (0.59 mL, 2.89 mmol, 3 eq.) was added to a solution of 2,4-dichloro-6,7-dimethoxyquinazoline **1** (0.25 g, 0.96 mmol, 1 eq.) in dry THF (5.5 mL) and the resulting mixture was stirred at room temperature for 24 hours until TLC showed that the starting material had disappeared. After filtration of the white salt, the filtrate was evaporated under reduced pressure and the resulting crude was triturated with petroleum ether, collected by filtration, and finally purified by a silica gel column eluting with a mixture AcOEt:MeOH (40:1) to get the intermediate **MC4120** as a white powder, yield 92%. M.p. 180-181°C: ^{1}H-NMR (400MHz; DMSO) δ ppm 1.63-1.72 (m, 2H, 2 x C*H* piperidine ring), 1.89-1.92 (m, 2H, 2 x C*H* piperidine ring), 2.05-2.11 (m, 2H, 2 x C*H* piperidine ring), 2.87-2.90 (m, 2H, 2 x C*H* piperidine ring), 3.51 (s, 2H, NCH_2Ph), 3.88 (s, 3H, OCH_3), 3.89 (s, 3H, OCH_3), 4.09-4.13 (broad, 1H, NHC$_4$-*H*-piperidine ring), 7.06 (s, 1H, C*H* quinazoline ring), 7.24-7.27 (m, 1H, C*H* phenyl ring), 7.31-7.36 (m, 4H, C*H* phenyl rings), 7.64 (s, 1H, C*H* quinazoline ring), 8.01 (d, 1H, N*H*). MS (ESI) 413 $[M + H]^+$. *N*-(1-Benzylpiperidin-4-yl)-2-chloro-6,7-dimethoxyquinazolin-4-amine **MC4120** (100 mg, 0.24 mmol, 1 eq.) was dissolved in 1 mL of isopropyl alcohol. To this solution was added 3-(dimethylamino)propylamine (67 µL, 0.52 mmol, 2.2 eq.) and the resulting solution was heated using microwave irradiation to 130°C for 4 hours and 30 minutes. After cooling, TLC indicated the completion of the reaction. After removal of the solvent by rotary evaporation, the residue was suspended in water (7 mL) and extracted with AcOEt (6 x 10 mL). The combined organic phases were then washed with brine (1 x 3 mL) and dried over Na_2SO_4. After filtration, the solvent was removed under vacuum and the product was purified by an alumina column eluting with a mixture AcOEt:MeOH (15:1) to afford **E11** as a white powder, yield 65%. M.p. 102-103°C: ^{1}H-NMR (400MHz; DMSO) δ ppm 1.64-1.73 (m, 4H, 2 x C*H* piperidine ring and NHCH$_2$CH_2CH$_2$N(CH$_3$)$_2$), 2.06-2.12 (m, 2H, 2 x C*H* piperidine ring), 2.28-2.31 (t, 2H, NHCH$_2$CH$_2$CH_2N(CH$_3$)$_2$), 2.92-2.95 (m, 2H, 2 x C*H* piperidine ring), 3.28-3.32 (m, 2H,

NHC*H*$_2$CH$_2$CH$_2$N(CH$_3$)$_2$), 3.57 (s, 2H, NC*H*$_2$Ph), 3.85 (s, 3H, OC*H*$_3$), 3.86 (s, 3H, OC*H*$_3$), 4.12-4.16 (broad m, 1H, NHC$_4$-*H*-piperidine ring), 6.19 (broad t, 1H, N*H*CH$_2$CH$_2$CH$_2$N(CH$_3$)$_2$), 6.71 (s, 1H, C*H* quinazoline ring), 7.22 (broad d, 1H, N*H*), 7.29-7.33 (m, 1H, C*H* phenyl ring), 7.35-7.41 (m, 4H, C*H* phenyl rings), 7.47 (s, 1H, C*H* quinazoline ring). MS (ESI) 479 $[M + H]^+$.

*Preparation of N^2-(3-(dimethylamino)propyl)-6,7-dimethoxy-N^4,N^4-dimethylquinazoline-2,4-diamine (**MC3767**).* A 2.0 M solution of dimethylamine in THF (2.03 mL, 4.05 mmol, 3 eq.) was added to a solution of 2,4-dichloro-6,7-dimethoxyquinazoline **1** (0.35 g, 1.35 mmol, 1 eq.) in dry THF (8.0 mL) and the resulting mixture was stirred at room temperature for 1 h 30 min until TLC showed that the starting material had disappeared. After filtration of the white salt, the filtrate was evaporated under reduced pressure and the resulting crude was triturated with petroleum ether, collected by filtration, and finally purified by a silica gel column eluting with a mixture AcOEt:Hexane (1:1) to get the intermediate **MC4121** as a white powder, yield 90%. M.p. 173-174°C: ^{1}H-NMR (400MHz; DMSO) δ ppm 3.32 (s, 6H, N(C*H*$_3$)$_2$), 3.89 (s, 3H, OC*H*$_3$), 3.90 (s, 3H, OC*H*$_3$), 7.12 (s, 1H, C*H* quinazoline ring), 7.40 (s, 1H, C*H* quinazoline ring). MS (ESI) 268 $[M + H]^+$. *N*-(Dimethyl)-2-chloro-6,7-dimethoxyquinazolin-4-amine **MC4121** (200 mg, 0.75 mmol, 1 eq.) was dissolved in 2.4 mL of isopropyl alcohol. To this solution was added 3-(dimethylamino)propylamine (0.11 mL, 0.90 mmol, 1.2 eq.) and sodium iodide (112 mg, 0.75 mmol, 1 eq.) and the resulting solution was heated using microwave irradiation to 130 °C for 3 h. After cooling, TLC indicated the completion of the reaction. After removal of the solvent by rotary evaporation, the residue was suspended in water (5 mL) and extracted with AcOEt (10 x 8 mL). The combined organic phases were then dried over Na_2SO_4. After filtration, the solvent was removed under vacuum and the product was purified by an alumina column eluting with a mixture AcOEt:MeOH (20:1) to afford **3** as a white powder, yield 60%. M.p. 65-66°C: ^{1}H-NMR (400MHz; DMSO) δ ppm 1.64-1.68 (m, 2H, NHCH$_2$C*H*$_2$CH$_2$N(CH$_3$)$_2$), 2.24-2.27 (t, 2H,

$NHCH_2CH_2CH_2N(CH_3)_2$), 3.13 (s, 6H, $N(CH_3)_2$), 3.29-3.31 (m, 2H, $NHCH_2CH_2CH_2N(CH_3)_2$), 3.79 (s, 3H, OCH_3), 3.84 (s, 3H, OCH_3), 6.32 (t, 1H, $NHCH_2CH_2CH_2N(CH_3)_2$), 6.75 (s, 1H, C*H* quinazoline ring), 7.14 (s, 1H, C*H* quinazoline ring). MS (ESI) 334 $[M + H]^+$.

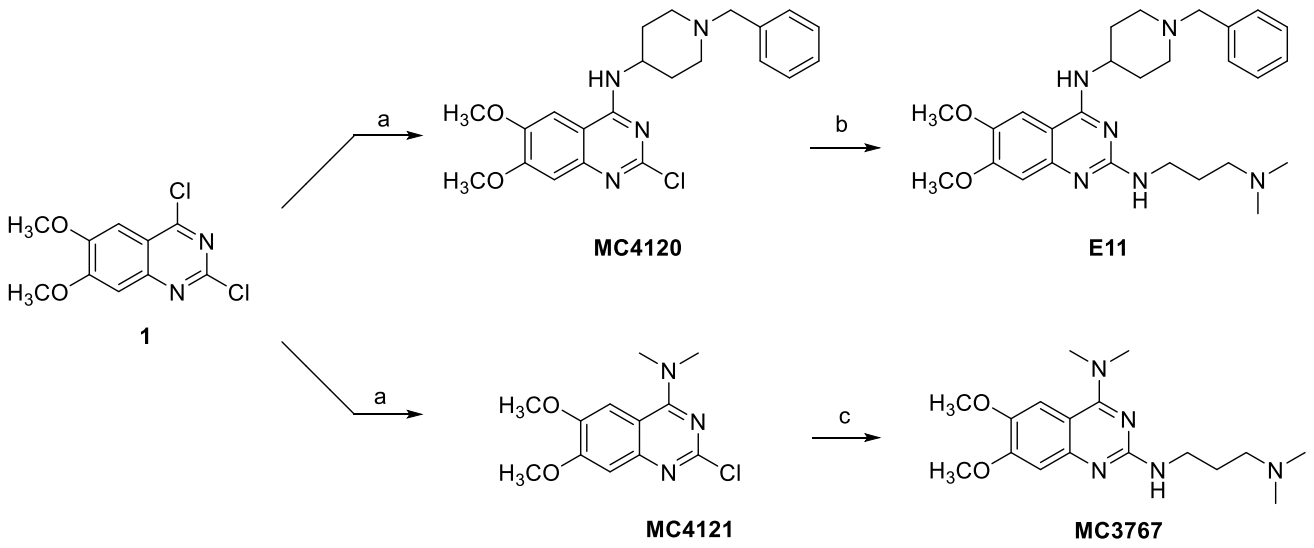

Reagents and conditions: (a) proper amine, dry THF, RT; (b) N^1,N^1-dimethylpropane-1,3-diamine, *i*-PrOH, microwave 130 °C; (c) N^1,N^1-dimethylpropane-1,3-diamine, NaI, *i*-PrOH, microwave 130 °C.

Supplementary Figures

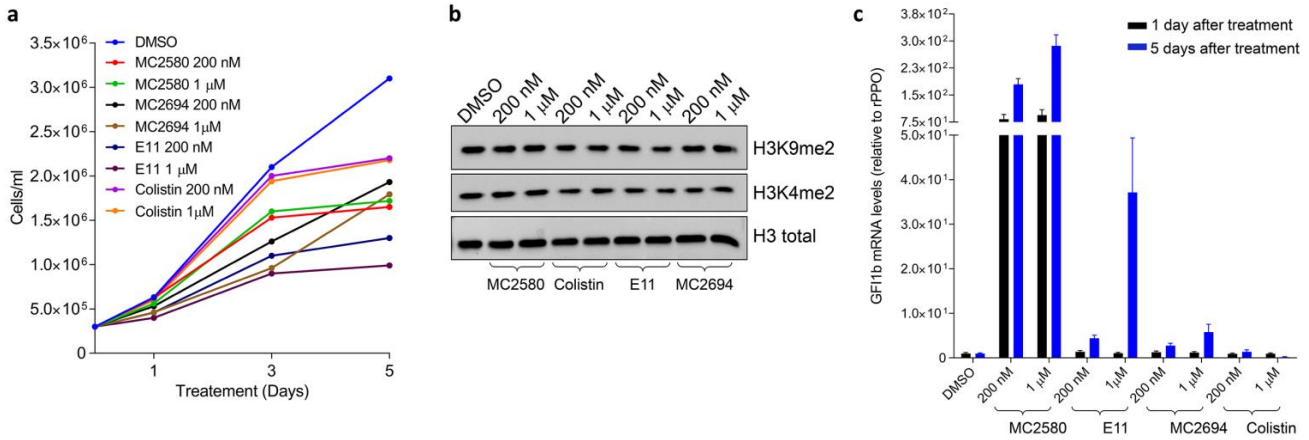

fig. S1. Cellular characterization of LSD1 inhibitors. Acute myeloid leukemia was chosen as model because LSD1 inhibitors are emerging as very attractive drugs against this hematological malignancy. Reference compound **MC2580** was chosen as positive control as it is a well-characterized potent LSD1 inhibitor. (**a**) **MC2580** arrests cell growth of MV4-11 cells by ≈ 50%, without clear dose dependence. Compound **MC2694** behaves similarly, while **E11** is stronger in inhibiting cell growth than reference **MC2580**. Polymyxin E (colistin) is instead a weaker inhibitor, although this observation might be due to reduced permeability. With increasing concentrations up to 50-times the measured K_d values (10 μM), compounds **MC2694** and **E11** showed 100% cytotoxic. These results indicated that the cyototoxicity is unlikely to be only caused by LSD1 inhibition but rather originates from a combination of effects, which might reflect also their activity on G9a. (**b**) Analysis of methylation levels of histone H3 Lysine 4 (H3K4me2) and Lysine 9 (H3K9me2) marks in leukemia MV4-11 cells upon treatment with reference inhibitor **MC2580**, polymixin E, and the two most potent quinazoline derivatives. None of the compounds induced any significant up-regulation of H3K4me2 over the baseline levels. (c) Transcriptional effect of quinazoline derivatives and polymyxin E (colistin) as tested by qPCR. Expression levels of *Gfi1-B* were analyzed as an established target of LSD1 in MV4-11 cells. At earliest time points (24h), reference compound **MC2580** is the only one able to increase expression, whereas at later time points (shown is 5 days treatment) also **E11** is able to induce significantly *Gfi1-B*.

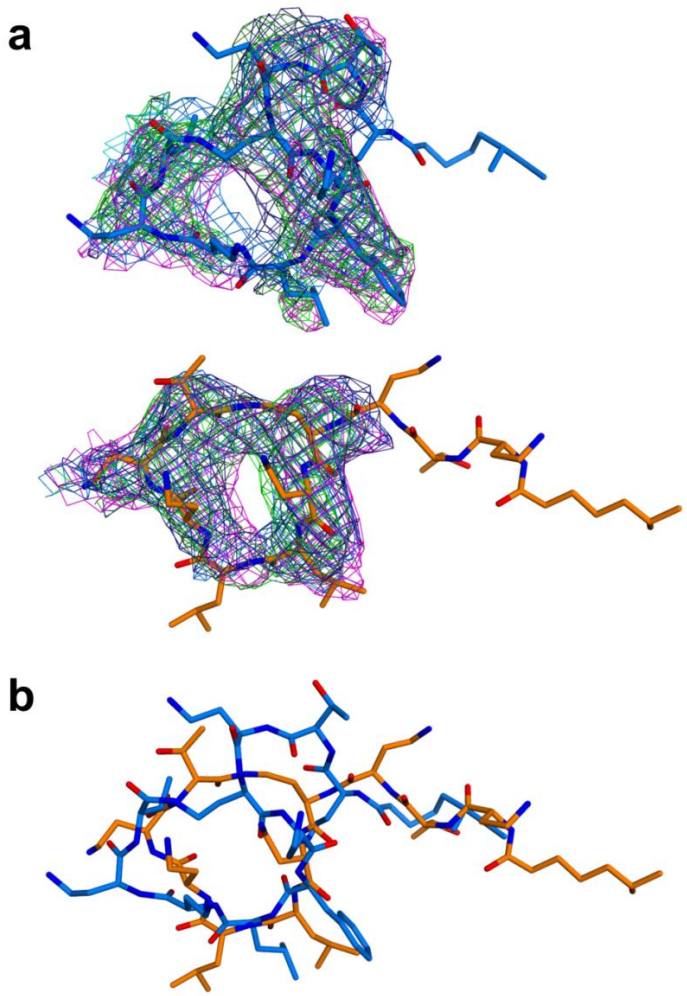

fig. S2. Comparison of polymyxin B and polymyxin E conformations from multiple data sets. (**a**) Superposition of $2F_o$-F_c experimental electron densities of polymyxins B and E from multiple data sets (see table S2). Polymyxin B (blue sticks) and E (orange sticks) central rings position in a well-defined electron density, whereas the extended aliphatic side chain is in a flexible conformation not visible in any of the collected data sets. Superpositions of electron density maps were generated using the CCP4 software SUPERPOSE for generation of rotation/translation matrices and MAPUTILS for map generation. (**b**) Superposition of polymyxins shows that the two antibiotics bind in a similar overall conformation.

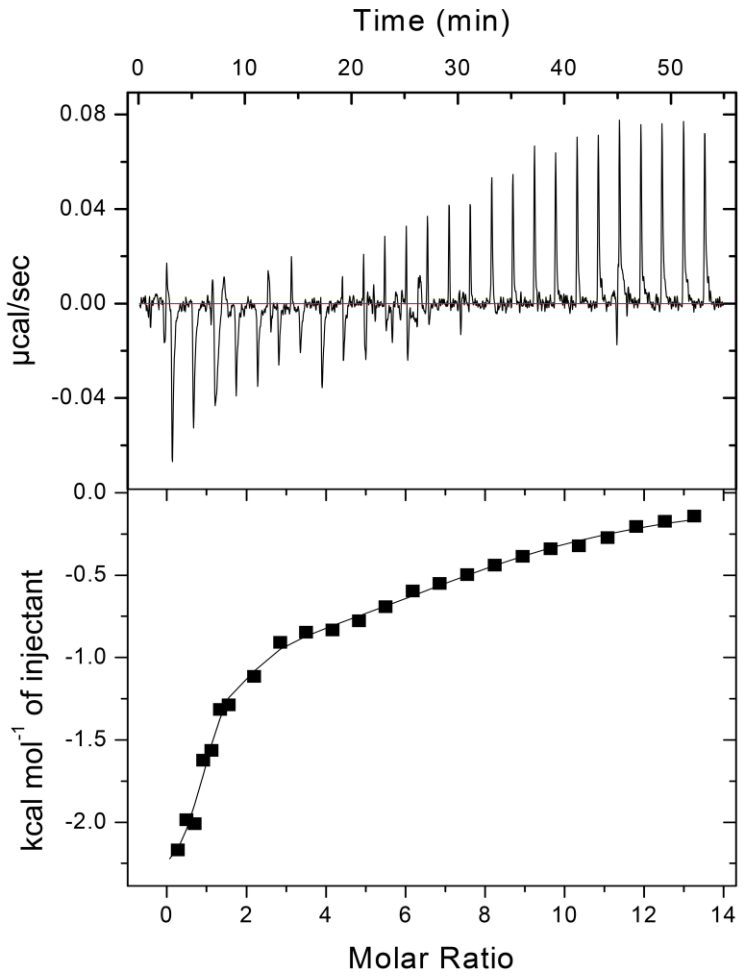

fig. S3. Characterization of the binding of E11 to LSD1-CoREST in solution by isothermal titration calorimetry. Calorimetric data of **E11** binding to LSD1-CoREST. Top panel shows the raw heat measured over a series of **E11** injections (1.5 mM). Each signal is integrated as data point and shown in the bottom panel.

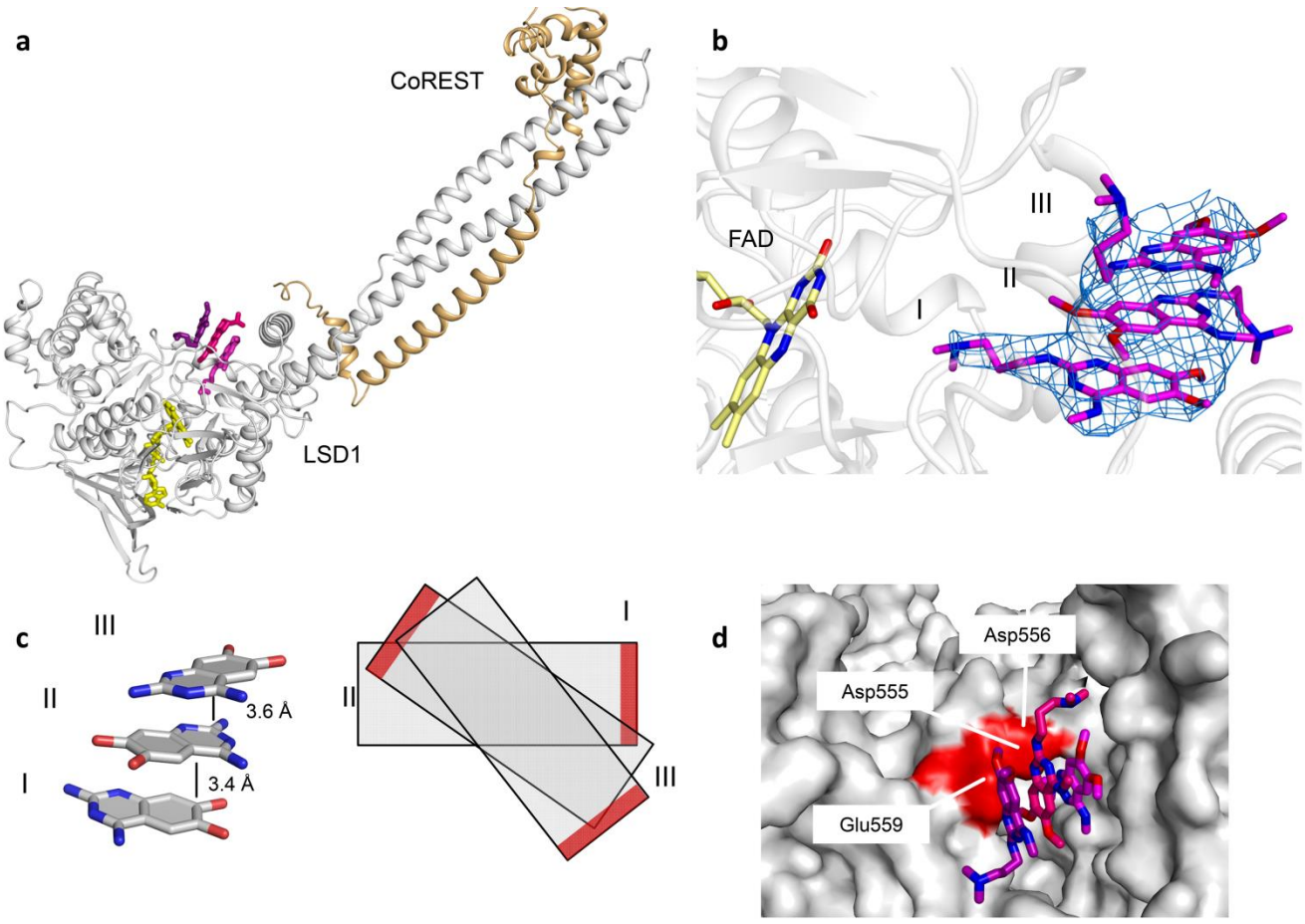

fig. S4. Noncovalent quinazoline-derived compound MC3767 binds the LSD1 active site in a multiple stacking assembly as E11. (**a**) A stack of three inhibitor molecules (magenta sticks) bind the active site of LSD1-CoREST (white and wheat cartoon, respectively) at > 5 Å from FAD (yellow sticks). (**b**) Side view of LSD1-CoREST complex with **MC3767**, showing the inhibitors at the entrance of the binding site. 2Fo-Fc electron density maps (1.2 σ level) are calculated before inclusion of the ligand in the refinement. (**c**) Simplified views of inhibitor molecules stacking in alternate flipped orientations, with an intermolecular distance of 3.8-4.0 Å (side view). Red bars on the right panel indicate the position of the methoxy groups in each ligand. (**d**) Surface highlight (red) of negatively charged residues of LSD1 that represent the primary binding region for quinazoline **MC3767**.

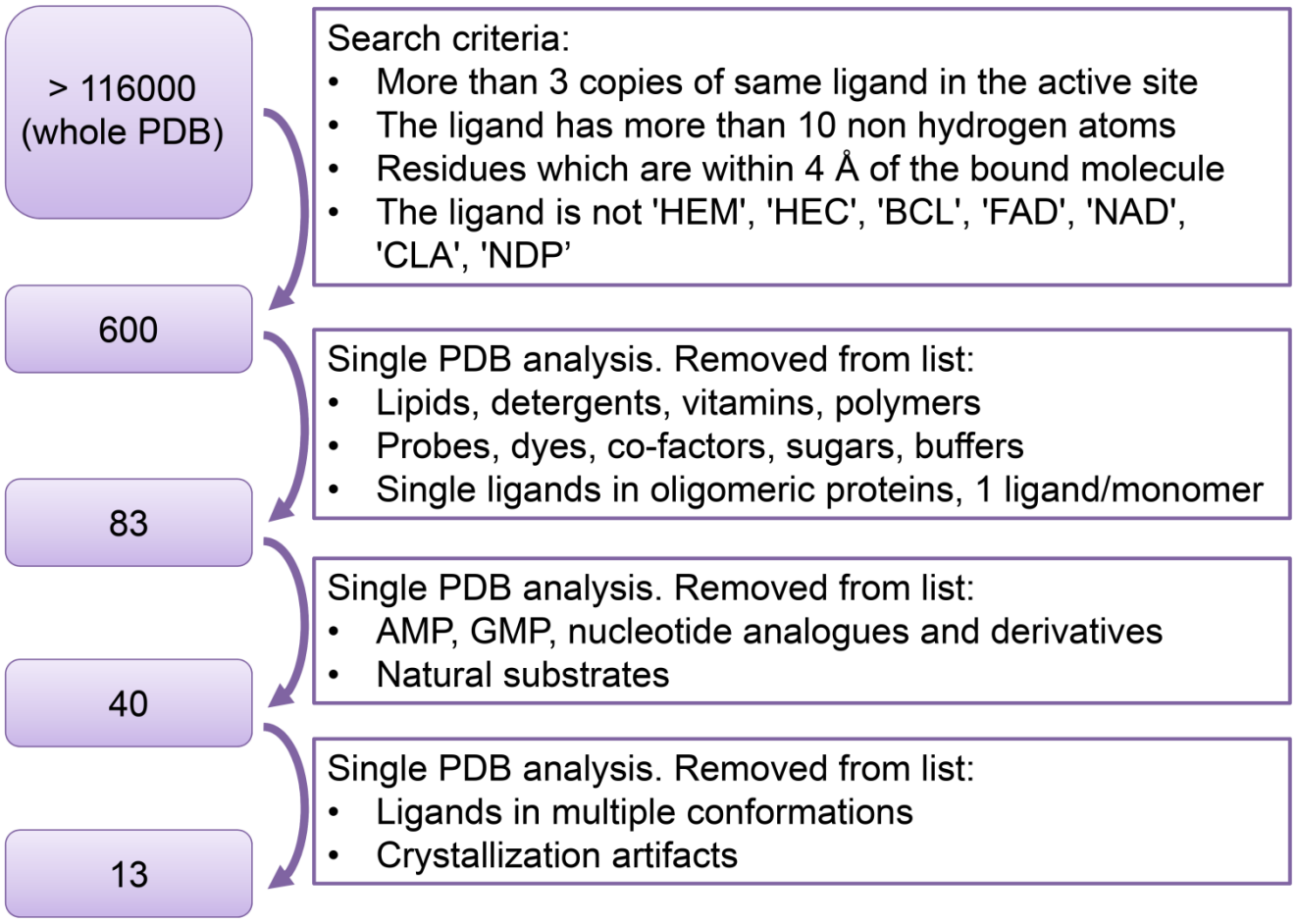

fig. S5. Workflow of the PDB search of multicopy stacking small-molecule inhibitors. Numbers in purple boxes refer to the number of PDB structures left for the analysis after each selection step (on the right).

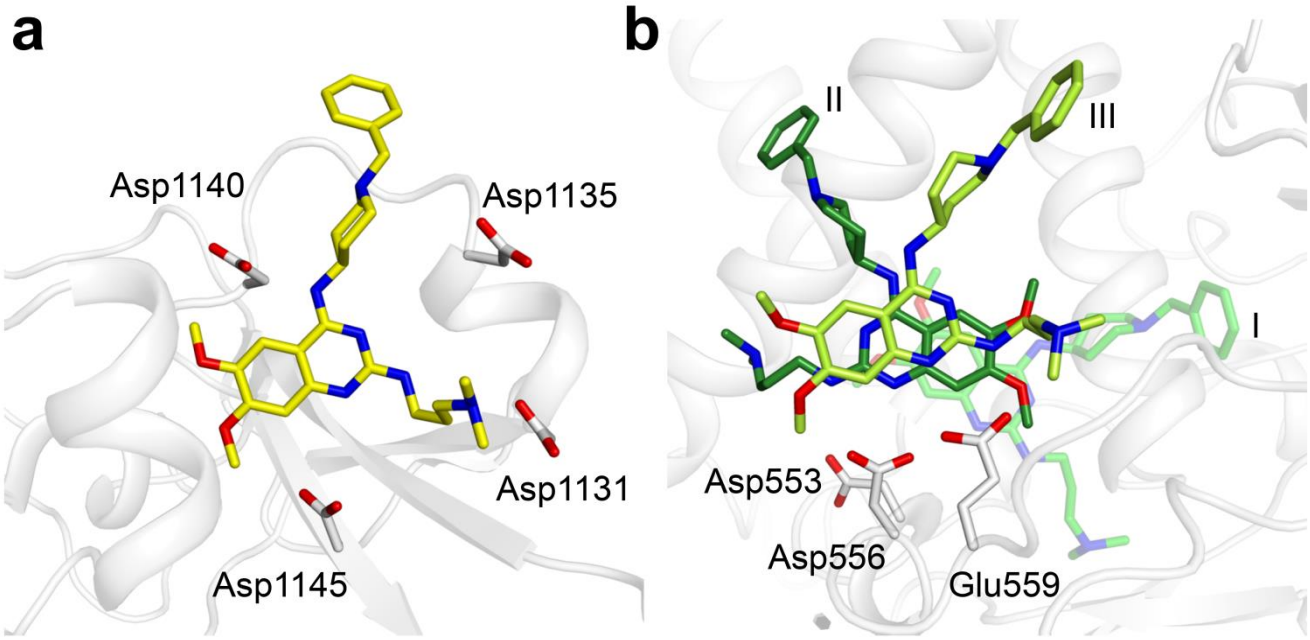

fig. S6. Comparison of histone methyltransferase G9a-like protein (GLP) and histone demethylase LSD1 in complex with compound E11. (**a**) GLP in complex with **E11** (PDB 3MO0), which binds in single copy. (**b**) LSD1-**E11** complex, where inhibitor binds in multiple stacking copies. For representation simplicity, ligands IV and V are omitted. Ligands are represented as green (I), forest (II) or lime (III) sticks.

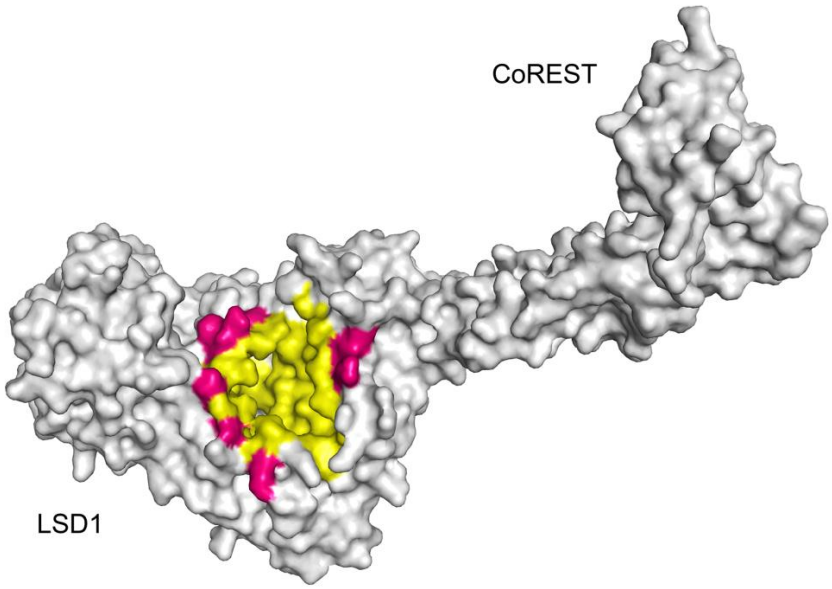

fig. S7. LSD1 druggable space is expanded by the binding of noncovalent compounds. Surface representation of LSD1-CoREST (white) and highlight of the extended druggable space (magenta) compared to all of the other LSD1 ligands previously characterized (yellow; table S4).

Supplementary Tables

table S1. Diffraction, data collection, and refinement statistics.

	E11 (5L3E)	MC3767 (5LBQ)	Polymyxin B (5L3F)	Polymyxin E (5L3G)
Data collection[*,†,‡]				
Space group	I222	I222	I222	I222
Cell dimensions				
a, *b*, *c* (Å)	116.6, 178.4, 233.8	120.1, 179.6 234.2	119.2, 179.0, 235.8	119.8, 179.5, 237.0
α, β, γ (°)	90.0, 90.0, 90.0	90.00, 90.00, 90.00	90.0, 90.0, 90.0	90.0, 90.0, 90.0
Resolution range (Å)	97.58 - 2.80 (2.87 - 2.80)	99.85 - 3.30 (3.45 - 3.30)	49.61 - 3.50 (3.69 - 3.50)	48.78 - 3.10 (3.21 - 3.10)
R_{merge}	0.134 (1.377)	0.191 (1.484)	0.161 (1.305)	0.069 (1.423)
$I / \sigma I$	8.3 (1.1)	5.7 (1.4)	7.7 (1.1)	11.6 (1.1)
Completeness (%)	99.8 (99.4)	100.0 (100.0)	99.9 (99.9)	99.7 (99.8)
Redundancy	5.0 (5.1)	5.3 (5.6)	4.7 (4.9)	3.5 (3.6)
Refinement[†]				
Resolution (Å)	2.80	3.30	3.50	3.10
No. unique reflections	60074 (4388)	38477 (4646)	32150 (4642)	46474 (4510)
R_{work} / R_{free}	0.208/0.227	0.233/0.244	0.186/0.210	0.172/0.197
No. atoms				
Protein	6293	6293	6293	6293
Ligands	229	122	138	136
Water	0	0	0	0
Average *B*-factors (Å^2)				
Protein	72	81	123	126
Ligands[§]	95	95	148	136
Water	-	-	-	-
R.m.s. deviations				
Bond lengths (Å)	0.013	0.011	0.014	0.015
Bond angles (°)	1.79	1.68	1.20	1.66

[*] For each structure, one crystal was used and 1 molecule was found in the asymmetric unit.

[†] Values in parentheses are for reflections in the highest-resolution shell.

[‡] The observed resolution limits of the diffraction data were selected by evaluating the mean(I) correlation between half-data sets, as defined by Karplus and Diederichs ***(39)***

[§] average B-factor calculation was carried out excluding all zero-occupancy atoms in the final PDB model.

table S2. Diffraction, data collection, and refinement statistics for all data sets of polymyxins B and E.
Data are available for download in the "movies and data" section of the http://www.unipv.it/biocry website. (Direct link to data set: http://www.unipv.it/biocry/data/Speranzini_et_al_LSD1-polymyxin_data.zip).

	Polymyxin B (5L3F)	**Polymyxin B (Data set 2)**	**Polymyxin B (Data set 3)**	**Polymyxin B (Data set 4)**	**Polymyxin B (Data set 5)**	**Polymyxin B (Data set 6)**
Data collection[*,†,‡]						
Space group	I222	I222	I222	I222	I222	I222
Cell dimensions						
a, *b*, *c* (Å)	119.2, 179.0, 235.8	119.5, 179.7, 236.1	119.6, 180.0, 236.3	120.6, 181.2, 236.5	118.8, 179.0, 235.6	120.4, 179.7, 235.3
α, β, γ (°)	90, 90, 90	90, 90, 90	90, 90, 90	90, 90, 90	90, 90, 90	90, 90, 90
Resolution range (Å)	49.61 - 3.50 (3.69 - 3.50)	49.34 - 3.00 (3.10 - 3.00)	49.51 - 3.10 (3.21 - 3.10)	49.52 - 3.40 (3.57 - 3.40)	48.83 - 3.10 (3.21 - 3.10)	49.22 - 3.20 (3.32 - 3.20)
R_{merge}	0.161 (1.305)	0.091 (1.599)	0.104 (1.379)	0.162 (1.777)	0.077 (1.322)	0.102 (0.888)
$I / \sigma I$	7.7 (1.1)	13.3 (1.1)	8.0 (0.8)	6.4 (1.0)	11.5 (0.9)	8.9 (1.4)
Completeness (%)	99.9 (99.9)	99.8 (98.5)	99.8 (99.8)	98.1 (98.1)	99.4 (99.5)	99.8 (99.6)
Redundancy	4.7 (4.9)	5.7 (5.7)	3.7 (3.7)	4.0 (3.9)	3.6 (3.5)	3.8 (3.8)
Refinement[†]						
Resolution (Å)	3.50	3.00	3.10	3.40	3.10	3.20
No. unique reflections	32150 (4642)	50914 (4583)	45783 (4444)	35264 (4623)	46272 (4504)	42346 (4366)
R_{work} / R_{free}	0.186/0.210	0.165/0.197	0.167/0.204	0.178/0.199	0.166/0.197	0.213/0.230
No. atoms	6431	6431	6429	6429	6429	6431
Protein	6293	6293	6289	6291	6289	6293
Ligands	138	138	140	140	140	138
Water	0	0	0	0	0	0
Average *B*-factors (Å^2)						
Protein	123	109	110	133	114	100
Ligands[§]	148	142	140	155	146	127
Water	-	-	-	-	-	-
R.m.s. deviations						
Bond lengths (Å)	0.014	0.011	0.010	0.010	0.010	0.015
Bond angles (°)	1.20	1.17	1.30	1.34	1.28	1.23

	Polymyxin E (5L3G)	Polymyxin E (Data set 2)	Polymyxin E (Data set 3)	Polymyxin E (Data set 4)	Polymyxin E (Data set 5)
Data collection[*,†,‡]					
Space group	I222	I222	I222	I222	I222
Cell dimensions					
a, *b*, *c* (Å)	119.8, 179.5, 237.0	120.4, 179.8, 235.9	118.8, 179.1, 238.0	119.4 178.2 235.4	118.8, 179.1, 238.0
α, β, γ (°)	90, 90, 90	90, 90, 90	90, 90, 90	90, 90, 90	90, 90, 90
Resolution range (Å)	48.78 - 3.10 (3.21 - 3.10)	49.31 - 3.20 (3.32 - 3.20)	49.56 - 3.10 (3.21 - 3.10)	49.10 - 3.30 (3.45 - 3.30)	49.22 - 3.50 (3.69 - 3.50)
R_{merge}	0.069 (1.423)	0.077 (1.005)	0.097 (2.000)	0.134 (1.375)	0.138 (1.271)
$I / \sigma I$	11.6 (1.1)	9.8 (1.3)	10.0 (0.9)	7.3 (1.2)	8.9 (1.6)
Completeness (%)	99.7 (99.8)	99.5 (99.8)	99.4 (99.8)	99.4 (99.4)	99.5 (99.5)
Redundancy	3.5 (3.6)	3.4 (3.6)	4.0 (4.1)	3.7 (3.8)	4.6 (4.9)
Refinement[†]					
Resolution (Å)	3.10	3.20	3.10	3.30	3.50
No. unique reflections	46474 (4510)	42284 (4394)	46019 (4503)	37819 (4559)	31434 (4536)
R_{work} / R_{free}	0.172/0.197	0.176/0.196	0.184/0.208	0.181/0.212	0.196/0.227
No. atoms	6429	6429	6429	6429	6429
Protein	6293	6293	6293	6293	6293
Ligands	136	136	136	136	136
Water	0	0	0	0	0
Average *B*-factors (Å^2)					
Protein	126	132	126	120	141
Ligands[§]	136	147	139	133	147
Water	-	-	-	-	-
R.m.s. deviations					
Bond lengths (Å)	0.015	0.009	0.009	0.009	0.004
Bond angles (°)	1.66	1.29	1.22	1.26	0.73

[*] For each structure, one crystal was used and 1 molecule was found in the ASU

[†] Values in parentheses are for reflections in the highest-resolution shell.

[‡] The observed resolution limits of the diffraction data were selected by evaluating the mean(I) correlation between half-sets, as defined by Karplus and Diederichs ***(39)***

[§] average B-factor calculation was carried out excluding all zero-occupancy atoms in the final PDB model.

table S3. List of protein-inhibitor structures displaying multiple stacking conformation identified from PDB search.

PDB ID	Protein	Ligand ID	Ligand name and type	Biological Assembly	Total ligand number per biological assembly	Stacking ligand copies per biological assembly	Reference
1WRL , 1WRK	Troponin C	TFP	Trifluoperazine (antipsychotic and antiemetic drug)	homodimer*	4	4	n.a. ‡
2A3A	Chitinase	TEP	Theophylline (respiratory diseases treatment)	monomer*	4	2	(*40*)
2D41	RNA-dependent RNA polymerase NS5B	SNH	Oligotiophene derivative (non-nucleoside inhibitor)	monomer*	2	2	(*41*)
2FIX	Fructose-1,6-bisphosphatase	870	Benzenesulfonamide analogue (allosteric inhibitor)	homotetramer*	4	2	(*42*)
2V0M	Cytochrome 3A4	KLN	Ketoconazole (antimitotic)	homotetramer*	8	2	(*43*)
3IPY	Deoxycytidine Kinase	B87	Oligotiophene derivative (cyclopentane analogue)	homodimer*	4	2	(*44*)
4BFQ	Acetylcholine binding protein	083	Isoquinoline derivative (antimycoplasmal agent)	homopentamer*	14	3†	(*22*)
4DBS	Aldo-keto reductase AKR1C3	0HV	Flufenamic acid analogue (small molecule antagonist)	monomer*	2	2	(*45*)
4JLJ, 4JLK	Deoxycytidine kinase	1NM, 1NO	Pyrimidine-thiazole derivatives (small molecule inhibitors)	homodimer*	4	2	(*46*)
4O4R	Norovirus RNA-dependent RNA-polymerase	20V	PPNDS (8'-disulfonic acid)	homohexamer*	12	2	(*47*)

* Analysis was performed using EBI PISA
† At the B-C subunit interface, only 2 molecules were found
‡ n.a. Not available

table S4. List of published LSD1 PDB structures in complex with ligands.

PDB ID	Ligand ID/Chain	Ligand type	Resolution (Å)	References
Irreversible inhibitors: covalent adduct on FAD				
2EJR, 2UXX, 2Z5U	F2N, FAJ, FAJ	Tranylcypromine	2.7, 2.7, 2.3	(***48, 49***)
2XAF, 2XAG, 2XAH, 2XAJ, 2XAQ, 2XAS	TCF, TCF, 3PL, TCA, M84, M80	Tranylcypromine analogues	3.25, 3.1, 3.1, 3.3, 3.2, 3.2	(***18***)
3ABT, 3ABU	2PF, 12F	Tranylcypromine analogues	3.2, 3.1	(***50***)
4UV8, 4UV9, 4UVA, 4UVB, 4UVC	D69, D70, D73, D51, D52	Tranylcypromine analogues	2.8, 3.0, 2.9, 2.8, 3.1	(***51***)
4UXN	M8A	Tranylcypromine analogue	2.9	(***52***)
2UXN	Chain E	Histone H3-derived peptide, modified	2.7	(***53***)
Reversible inhibitors: substrate mimic				
2V1D	Chain C	Histone H3-derived peptide	3.1	(***6***)
2Y48	Chain C	SNAIL1-derived peptide*	3.0	(***25***)
3ZMS, 3ZMT, 3ZMU, 3ZMV, 3ZMZ, 3ZN0, 3ZN1	Chain C	SNAIL1 and INSM1-derived peptides*,†	3.0, 3.1, 3.2, 3.0, 3.0, 3.0, 2.8, 3.1	(***54***)
Reversible inhibitors: newly identified compounds				
5L3E	E11	Small-molecule inhibitor	2.8	This work
5LBQ	767	Small-molecule inhibitor	3.3	This work
5L3F	Chain C	Cyclic peptide	3.5	This work
5L3G	Chain C	Cyclic peptide	3.1	This work
Non-competitive inhibitors: nucleic acid				
4XBF	Chain D	RNA oligonucleotide	2.8	(***55***)

* SNAIL1, zinc finger transcription factor SNAI1

† INSM1, Insulinoma-associated protein 1, transcription regulator